applied sciences

MDPI

Article

Fiber Bragg Grating (FBG) Sensors in a High-Scattering Optical Fiber Doped with MgO Nanoparticles for Polarization-Dependent Temperature Sensing

Carlo Molardi [1], Tiago Paixão [2], Aidana Beisenova [1], Rui Min [3,4], Paulo Antunes [2], Carlos Marques [2], Wilfried Blanc [5] and Daniele Tosi [1,6,*]

1 School of Engineering, Nazarbayev University, 53 Kabanbay Batyr, Astana 010000, Kazakhstan
2 Physics Department & I3N, University of Aveiro, 3810-193 Aveiro, Portugal
3 Intelligent Manufacturing Faculty, Wuyi University, Jiangmen, China
4 ITEAM Research Institute, Universitat Politècnica de València, 46022 València, Spain
5 INPHYNI–CNRS UMR 7010, Université Côte d'Azur, Parc Valrose, 06108 Nice, France
6 Laboratory of Biosensors and Bioinstruments, National Laboratory Astana, 53 Kabanbay Batyr, Astana 010000, Kazakhstan
* Correspondence: daniele.tosi@nu.edu.kz

Received: 3 July 2019; Accepted: 30 July 2019; Published: 1 August 2019

Featured Application: Inscription and interrogation of fiber Bragg gratings into MgO nanoparticle-doped fiber for optical fiber distributed and multiplexed sensing.

Abstract: The characterization of Fiber Bragg Grating (FBG) sensors on a high-scattering fiber, having the core doped with MgO nanoparticles for polarization-dependent temperature sensing is reported. The fiber has a scattering level 37.2 dB higher than a single-mode fiber. FBGs have been inscribed by mean of a near-infrared femtosecond laser and a phase mask, with Bragg wavelength around 1552 nm. The characterization shows a thermal sensitivity of 11.45 pm/°C. A polarization-selective thermal behavior has been obtained, with sensitivity of 11.53 pm/°C for the perpendicular polarization (S) and 11.08 pm/°C for the parallel polarization (P), thus having 4.0% different sensitivity between the two polarizations. The results show the inscription of high-reflectivity FBGs onto a fiber core doped with nanoparticles, with the possibility of having reflectors into a fiber with tailored Rayleigh scattering properties.

Keywords: Fiber Bragg Grating (FBG); Rayleigh scattering; FBG sensor; enhanced backscattering fiber; polarization-sensitive device

1. Introduction

A Fiber Bragg Grating (FBG) is a periodic modulation of the refractive index within the core of an optical fiber [1], which results in a wavelength-selective resonant behavior that resonates at the so-called Bragg wavelength [2]. The spectrum of an FBG results in a narrow bandwidth of reflected waves, while the remainder of the spectrum is transmitted through the grating. The FBG, as well described in [1,2], implements the Bragg resonant condition within an optical fiber, and results in a compact device that finds broad applications in telecommunications and sensing. In fiber optics, FBGs are extremely important as they behave as narrow-band notch filters, or as passband filters when preceded by a circulator or fiber coupler [3]. An FBG substantially implements a similar function to microwave or electronic resonators, but at a much narrower resonance filters and at infrared wavelengths. Thus,

FBGs find many applications in telecommunications [1], in signal equalization [3], and as reflectors for laser cavity in fiber lasers [4]. FBGs are also popular for sensing, as the Bragg wavelength shifts when temperature or strain variations are applied to the grating [5], making it a compact sensing device that finds numerous fields of application.

The first generation of FBGs have been fabricated using photosensitive fibers [1], having a significant Ge-doping that facilitates the process of FBG inscription, and on standard single-mode fibers (SMFs) by means of H_2 loading [6]. More recently, the possibility to use a femtosecond (fs) laser focused on the fiber core has opened the possibility of inscribing an FBG on several types of fibers [7,8]. SMF fibers have low attenuation and adhere to telecommunication standards (such as ITU-T G.657.A1 and G.652.D), and the possibility of inscribing FBGs into such fibers gives rise to wavelength filters and sensors at a relatively low cost, and easy to be interconnected.

With the emergence of research on specialty fibers, engineered in order to achieve specific functions that SMFs cannot achieve, new sensing functions can be enabled. In this sense, the possibility of inscribing FBGs in specialty fibers has provided the backbone for advanced applications in sensing and fiber lasers, particularly thanks to direct inscription. Among others, Iadicicco et al. [9] reported FBGs in microstructured fibers which add refractive index sensitivity to the inherent temperature/strain sensitivity; Jovanovic et al. [10] reported FBGs directly inscribed with a point-by-point technique in the inner core of a dual-core fiber, which represents the end reflectors of a fiber laser cavity; Leal-Junior et al. [11] reported FBGs inscribed in a polymer fiber in the infrared, which achieves a much larger sensitivity to temperature effects, and reports also a humidity sensitivity; Pugliese et al. [12] reported FBGs inscribed in a bioresorbable fiber, which has the property of being potentially absorbed by the human body after use.

Among the specialty fibers used in sensing applications, several efforts have been recently devoted to altering the Rayleigh scattering properties of fibers. In this scenario, three main approaches have given similar results. Yan et al. [13] reported a method based on rapid pulses with a fs laser (300 nJ at 250 kHz repetition rate), increasing the scattering level of a SMF by up to 45 dB. Parent et al. [14] have obtained similar results, with a scattering increment of 37 dB, by means of exposure to intense ultraviolet light; this method has also been used to generate random gratings [15]. More recently, Beisenova et al. [16] have obtained a 36.5 dB scattering increment by using a MgO-nanoparticle-doped (MgO-NP) fiber as sensing medium. This setup has also been used to design a scattering-level multiplexing [16,17], a new domain of multiplexing where the diversity is given by the scattering level at each sensing point. While the first two methods are characterized by a specific fabrication at one specific sensing point, the third method provides an optical fiber that can be spooled and spliced directly to a SMF, making the operation of building a multi-fiber sensing network much simpler.

The possibility to increase the scattering of a fiber is intriguing in distributed sensing, particularly using optical backscatter reflectometry (OBR) [18], whereas the analyzer detects the distributed Rayleigh scattering backreflection occurring in each region of the fiber. In such system, by increasing the Rayleigh scattering a larger signal at the analyzer can be obtained [13–17], over 3–4 orders of magnitude larger when properly tuning scattering properties.

In this work, the characterization of FBGs on a high-scattering MgO-NP fiber is presented. The possibility to have an FBG on such fiber opens important applications for sensing, as it allows tagging a specific sensing point as reference and measuring a sensing region relatively to the FBG. Also, due the polarization-sensitive behavior of the fiber, a different sensitivity for each polarization state can be observed. In the following, the experimental results of FBG inscription into a MgO-NP and the characterization of the grating for thermal effects, including a polarization-sensitive analysis, will be reported.

2. Fabrication and Setup

2.1. MgO Nanoparticle-Doped Fiber

The fiber used in this work presents a core doped with a random pattern of nanoparticles whose composition is based on MgO [17,19]. The fiber, designed to improve the efficiency of C-band optical amplifier (wavelengths from 1530 to 1565 nm), presents an additional doping of erbium in the core. The fiber possesses the typical telecom size, i.e., core diameter of 10 µm and cladding diameter of 125 µm, and a protective jacket with 250 µm diameter. This fact permits simple splicing operation with standard SMF-28 pigtails. The preform of the fiber has been fabricated by a conventional Modified Chemical Vapor Deposition (MCVD) process, a common technique for specialty optical fibers fabrication.

The proposed technology allows one to grow in-situ oxide nanoparticles due to high temperatures reached during the MCVD process [19] The implemented principle is based on the spontaneous phase separation process. This process involves the immiscibility of silicate compound that contain alkaline earth ions (MO, where M = Mg, Ca or Sr). The result is that the compound will decompose into two phases: one silica-rich and one MgO-rich in shape of spherical particles. The characteristics of the nanoparticles (size, size distribution) depends on the concentration of Mg, but typically the process generates nanoparticle whose size, location and refractive index are random. The size is in between 20 nm and 100 nm, while the refractive index is in between 1.53 to 1.65. The presence of nanoparticle strongly enhances the scattering and the losses [17,18].

2.2. Fiber Bragg Grating Inscription

The inscription of FBGs on the MgO-NP fiber has been carried out by means of a fs laser and phase mask method [10,11] [20], using the setup sketched in Figure 1a. The optical fiber has been placed between two fiber holders, leaving the stripped MgO-NP fiber section exposed to the phase mask area. With this setup, two FBGs have been inscribed, at 3 cm distance from each other. The first FBG has 2 mm length, and Bragg wavelength of 1538.5 nm (phase mask with a pitch of 1061 nm) at room temperature; the second FBG has 4 mm length, and Bragg wavelength around 1552.2 nm (phase mask with a pitch of 1072 nm) at room temperature. The spectrum of the second FBG, the one used in the spectral and polarization analysis, is reported in Figure 1b.

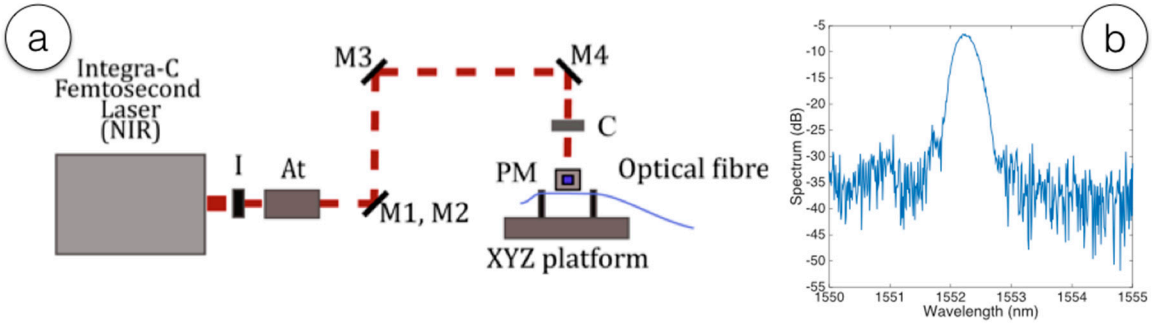

Figure 1. (**a**) Schematic diagram of the laser inscription setup used to inscribe refractive gratings; I—iris, At—power attenuator, M—mirror, C—Convex cylindrical lens, PM—Phase mask. (**b**) Spectrum of the FBG inscribed on the MgO-NP having Bragg wavelength around 1552.2 nm.

2.3. Experimental Characterization Setup

The analysis of FBG spectra, as well as of the MgO-NP fiber, has been performed using a commercial OBR analyzer (Luna OBR4600, Luna Inc., Roanoke, VA, USA). The setup used in measurements is shown in Figure 2, including both a schematic diagram and the photograph of the whole system. The MgO-NP fiber has been spliced to a lead-in SMF span by means of a standard splicer (SMF-SMF splicing recipe, cladding alignment, Fujikura 12-S, Tokyo, Japan). The OBR has been used with the following parameters: wavelength range 1525.0–1610.5 nm, resolution bandwidth 1.29 GHz (10.3 pm),

8192 wavelength points, no gain for each detector; the OBR spatial resolution is 9.8 µm. The OBR detects both polarizations, here labelled S (perpendicular) and P (parallel), where the orientation is referred to the swept laser of the OBR source [21].

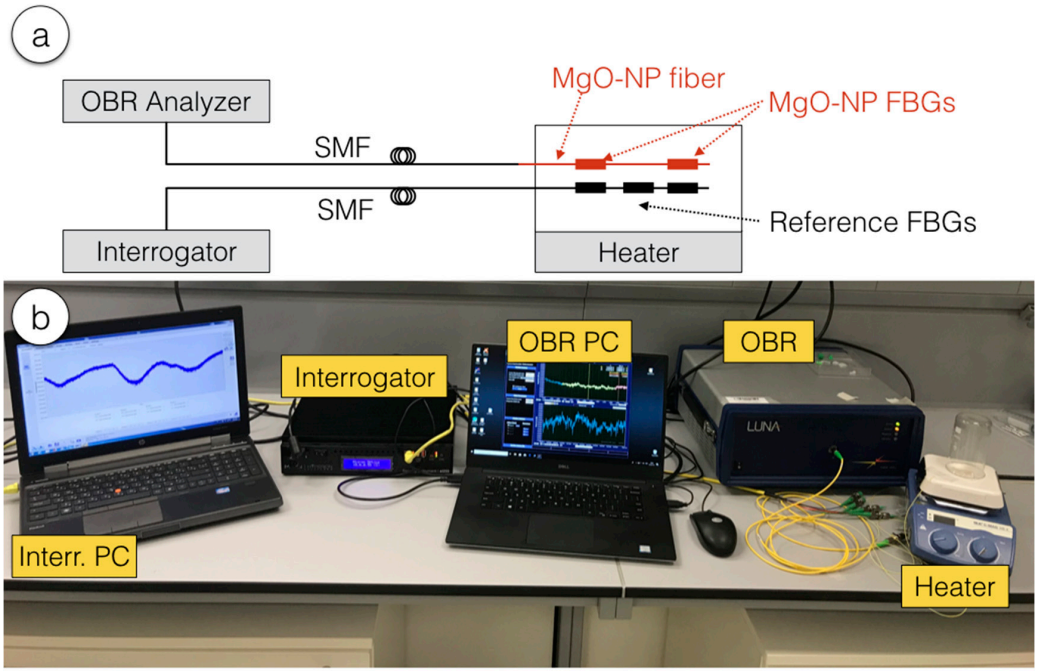

Figure 2. Setup of the FBG interrogation system. (**a**) Schematic diagram of the setup; (**b**) photograph.

Thermal variations have been obtained by placing the fiber in contact with a heating plate (C-MAG HS4, IKA, Staufen, Germany). The reference temperature has been measured by another FBG (ormoceramic draw-tower grating DTG-1550 nm, FBGS International, Geel, Belgium) connected to a commercial FBG interrogator (si255, 1 kHz, Micron Optics, Atlanta, GA, USA) and detecting the peak wavelength with ~0.1 pm accuracy; the thermal sensitivity of the reference FBG is 10.4 pm/°C. The hot plate temperature has been varied from 60°C to 145°C, approximately 40–125°C over the room temperature of 20°C. In order to maintain a heat uniformity, we the hot plate has been covered with a beaker.

3. Experimental Results

3.1. Characterization of Fiber Bragg Grating

The result of FBGs inscription on the MgO-NP fiber is shown in Figure 3, which displays the power backreflected at each section of the fiber for both polarizations. The lead-in fiber is a SMF, which has a scattering level around −91 dB and terminates at 4.58 m length (measured from the OBR lead-out connector). In the MgO-NP section, we observe a scattering gain, which is the increment of scattering with respect to the SMF, of 37.2 dB, similar to [17]. Due to the high scattering, the fiber has a high two-way loss estimated as 22.1 dB/m, i.e., cumulating both the forward and backward wave.

Two FBGs have been inscribed at the lengths of 4.60 m and 4.63 m. The first FBG exhibits a signal increment of ~10 dB over the scattering level and corresponds to a relatively weak FBG; the second FBG is stronger (28 dB over the scattering trace) and represents a strong FBG. We also observe that the polarization appears to fluctuate along the MgO-NP fiber, as previously observed in [22].

We report in Figure 4 the reflection spectrum of the stronger of the two MgO-NP FBGs, i.e., the grating inscribed at the length of 4.63 m as the temperature increases; the results are similar to the FBG inscribed at 4.60 m. The reflection spectrum of the FBG appears as ~28 dB over the noise floor, in compliance with Figure 3. As for a standard FBG, the spectrum appears to shift towards longer

wavelengths as the temperature variation ΔT increases from the reference value, maintaining the spectral shape. At the initial temperature (ΔT = 0 °C, corresponding to the room temperature) the Bragg wavelength is 1552.2 nm, and rises to 1553.6 nm for ΔT = 125.6 °C, at the maximum temperature.

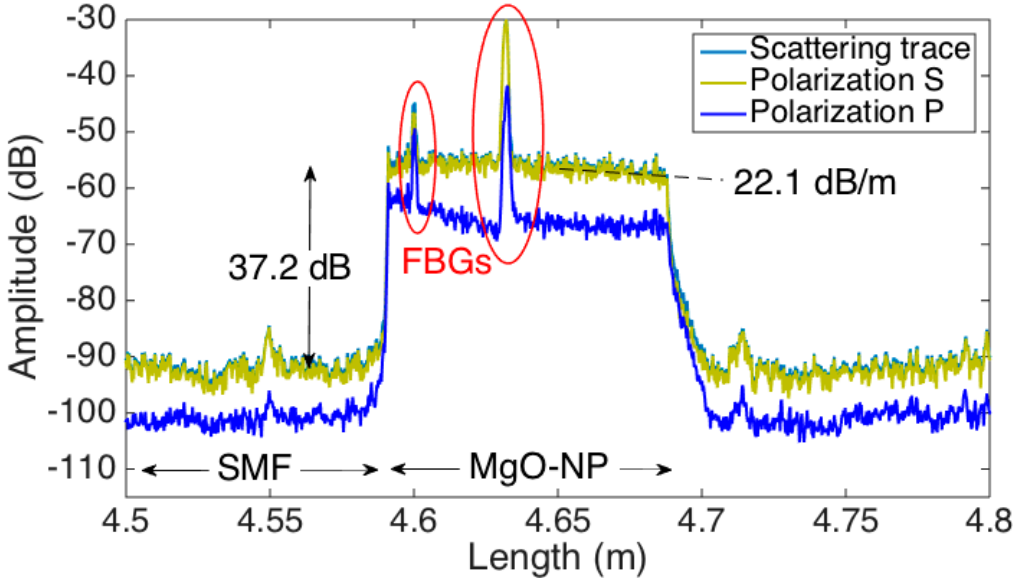

Figure 3. Backreflected signal for from the MgO-NP fiber with 2 FBGs inscribed at 4.60 m and 4.63 m.

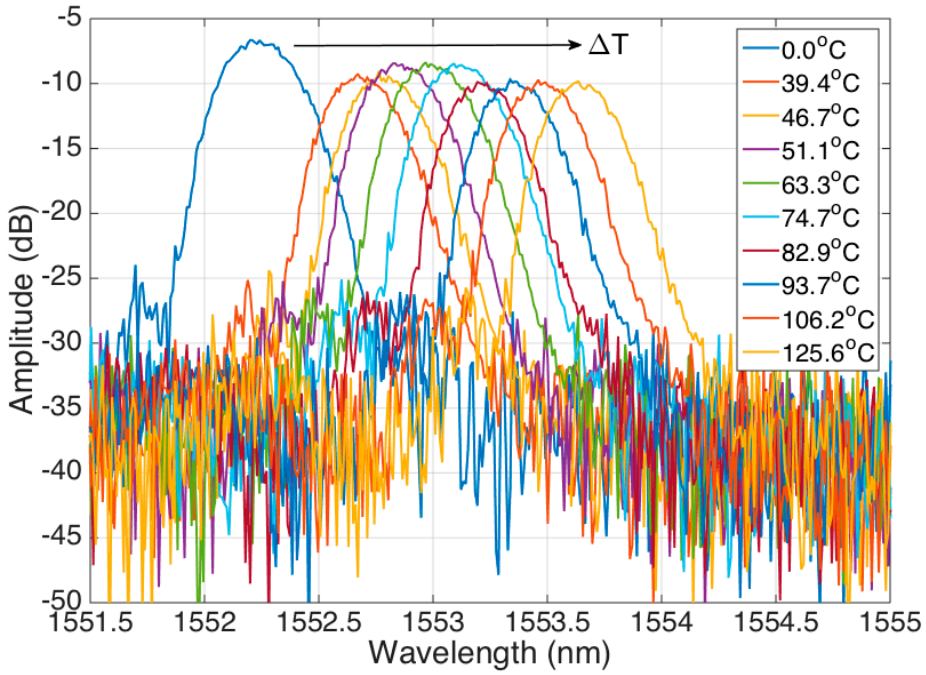

Figure 4. Reflection spectra of the MgO-NP FBG, for different values of temperature variation ΔT; the reference temperature ΔT = 0 °C corresponds to room temperature.

Figure 5 reports the Bragg wavelength of the FBG as a function of the temperature variation. As in [1,5], the FBG shows a linear wavelength shift, with sensitivity equal to 11.45 pm/°C and reference wavelength of 1552.262 nm; the fit has coefficient of determination R^2 = 0.997, which shows a very accurate fit for over 125°C of temperature range.

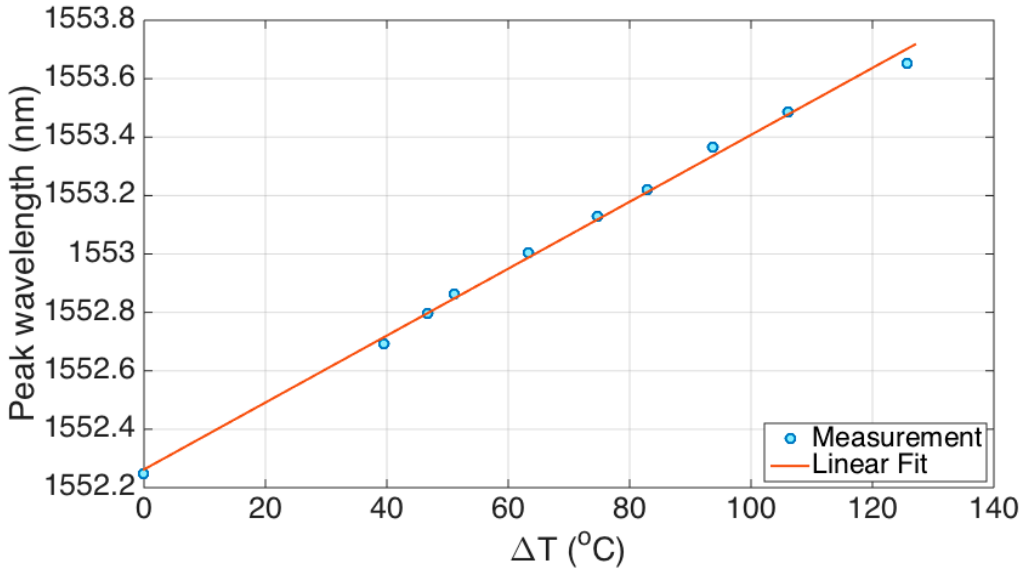

Figure 5. Bragg wavelength of the MgO-NP FBG as a function of the temperature variation. The chart shows the measured data and the linear fit (11.45 pm/°C, R^2 = 0.997).

3.2. *Polarization Analysis*

As previously outlined in [22], the MgO-NP fiber induces a beat length of polarization that has a higher frequency than a standard SMF, with polarization switching every few centimeters. This effect is common with the other methods proposed for enhancing the Rayleigh backscattering of the fiber [13–15]. Thus, in this section we investigate the polarization-sensitive behavior of the FBG, by separating the S/P polarizations into the analysis.

The polarization effects are shown in Figure 6, which reports the FBG spectra for S and P polarizations. At first, we observe a different amplitude between the two spectra, with the S polarization having a higher value, but also fluctuating as the temperature increases. The spectra for the polarization P appear narrower in bandwidth, and as temperature increases we observe that the spectra at the P polarization take a different wavelength shift than the spectra for the polarization S.

We can analyse independently the two polarizations, and determine the sensitivity to temperature at each wavelength; this analysis is shown in Figure 7. We observe a linear pattern for both polarizations, with thermal sensitivity of 11.53 pm/°C for the polarization S (R^2 = 0.997) and 11.08 pm/°C for the polarization P (R^2 = 0.995). The analysis shows a significant deviation between the two polarizations, as the sensitivity for the S polarization (the dominant one, given its higher amplitude) is 4.0% higher than for the P polarization; this is a reliable measurement given the fidelity of the linear fit, as the R^2 term is higher than 0.99 for both estimates. At room temperature, the Bragg wavelength is higher for the polarization P and lower for the S; as temperature increases however we see a progressive divergence between the Bragg wavelengths for both polarization states.

A polarization analysis is carried out in Figure 8, reporting the FBG bandwidth (estimated as the full-width half-maximum, FWHM) and the maximum spectral amplitude for each polarization. At first, we observe an interesting pattern for the FWHM, which at room temperature is wider for the P polarization (as shown in Figure 6) where the minimum amplitude is recorded; as the temperature increases, the FWHM assumes different values for the 2 polarization, and is equal to 0.33–0.35 nm for the S polarization and to 0.27–0.28 nm for the P polarization, showing a significant deviation which is also clear as the spectra are plotted in Figure 6.

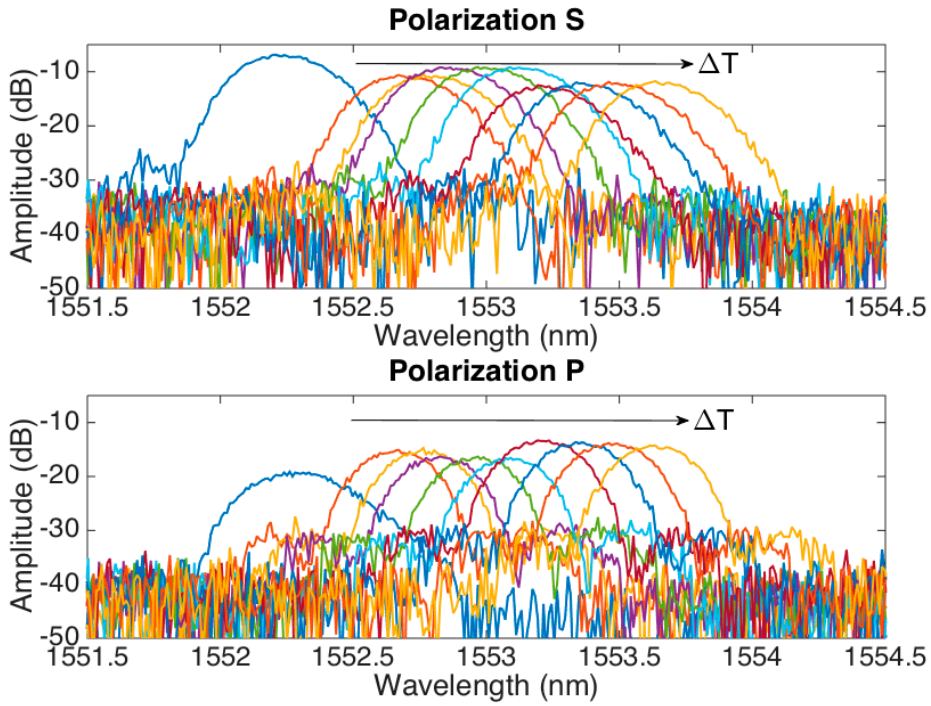

Figure 6. Reflection spectra of the FBG on MgO-NP fiber, evaluated for S (**upper**) and P (**lower**) polarizations.

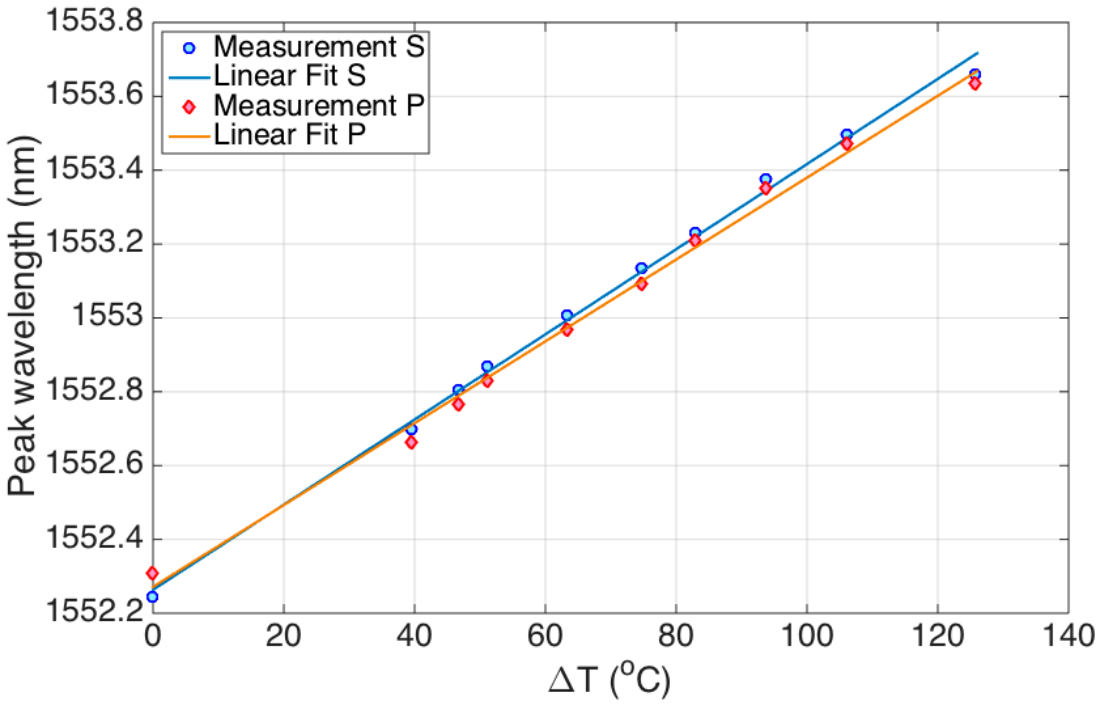

Figure 7. Bragg wavelength for each polarization as a function of the temperature variation.

The amplitude of the spectral response also shows a temperature-dependent pattern, as the light appears to transfer from the S to P polarization as the temperature increases. At room temperature, the polarization difference is over 12 dB, but reaches a minimum of 0.6 dB at $\Delta T = 75$ °C, where the two polarizations have similar amplitude; at higher temperature, the process reverses and S polarization appears to have higher amplitude.

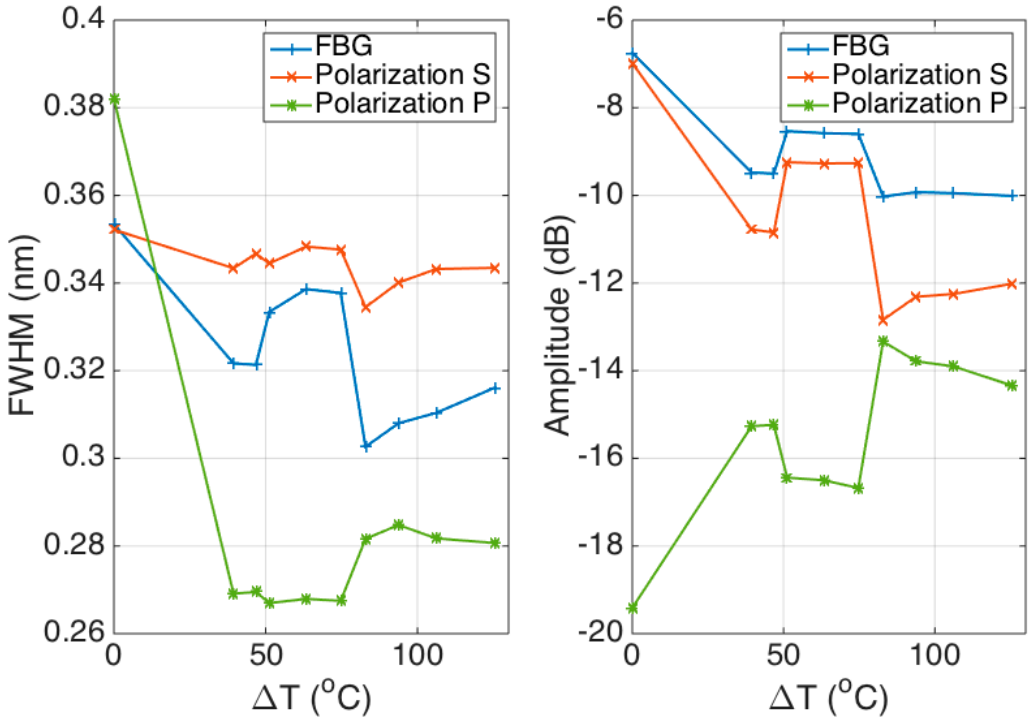

Figure 8. Polarization analysis of the FBG parameters: the chart reports the FWHM (**left**) and the maximum amplitude (**right**) of the FBG spectra at different temperature values, for the whole FBG and for each polarization independently.

4. Discussion

The characterization of FBGs on a high-scattering MgO-NP fiber, with enhanced backscattering properties, has implications, particularly in terms of sensing and polarization effects, as it can provide an additional layer of complexity in sensing.

The main difference between the MgO-NP fiber and the other methods for enhancing the backscattering is that the first one can be used, effectively, as a fiber, and thus the FBG is part of the optical circuitry used to implement filtering and cavity effects [4,10], as well as to create distributed reflectors supported by the random effect of the scattering nanoparticles [23]. In sensing, this is important as the FBG allows "tagging" a specific sensing point where the FBG is located, and referencing the remainder of the fiber to the valued measured in this location, enabling solutions that mix optical frequency domain reflectometry of fiber scattering and FBG interrogation [24,25]. The main application for the MgO-NP fiber is in scattering-level multiplexing, which requires a fiber with high Rayleigh scattering in order to simultaneously detect multiple channels on the OBR device [16,17]. The addition of FBGs to this sensing system can be used to extend the sensing length of each channel, by using the additional reflectivity of the FBG in addition to the scattering level, compensating for the relative inline high losses of the fiber.

In addition, the different sensitivity exhibited by the polarizations to thermal effects is a significant effect, as the difference is estimated as 4% with a good degree of confidence ($R^2 > 0.99$). In comparison, this difference is 0.5% for a fiber doped with MgO nanoparticles but having no scattering enhancement, and is <0.1% for a standard FBG [1].

Similar results have been obtained with FBGs inscribed on fibers having high birefringence [26,27] or on polarization-maintaining fibers [8], whereas it is clearly possible to distinguish between the two Bragg wavelengths of slow/fast axis. In this work, however, we do not use a fiber with asymmetric design, but rather the polarization effect happens due to the scattering events occurring in the fiber, which determine the S/P polarizations to have a different thermal coefficient. This effect has been used in birefringent fibers to discriminate strain and temperature by means of detecting the difference

between the two Bragg wavelengths, which is ~0.5 nm in [28]. It is noteworthy that the polarization effect is not obtained by asymmetrical design of the fiber [29], but is routed in the scattering content of the MgO nanoparticles. Overall, the results presented in this work open the possibility to thermally tune the wavelength and polarization of the FBGs inscribed on this fiber, considering also the different bandwidth exhibited by the two polarization states.

5. Conclusions

The characterization of FBGs onto a specialty fiber doped with MgO nanoparticles having enhanced Rayleigh scattering is reported in this work. The MgO-NP fiber has 37.2 dB scattering increment over a SMF, and 22.1 dB/m two-way loss. The FBGs achieved up to 28 dB amplitude over the scattering level. A thermal characterization shows the sensitivity to be 11.45 pm/°C, similar to standard glass fibers; the thermal sensitivity exhibits a 4% difference between the two S/P polarizations (respectively, 11.53 pm/°C and 11.08 pm/°C). Future work will consist on exploiting the polarization properties for sensing applications, and on the analysis of the high-scattering impact in FBG sensing networks.

Author Contributions: C.M., C.M., W.B., and D.T. conceptualized the work; W.B. fabricated the optical fiber used in experiments; T.P., P.A., R.M., and C.M. inscribed Bragg gratings into the fiber; C.M., A.B. prepared the characterization setup; C.M., A.B., D.T. performed the characterization of the Bragg gratings; C.M., C.M., W.B., D.T. analyzed and prepared the data; D.T., C.M., W.B., C.M., wrote the article; all authors reviewed data and manuscript.

Funding: This work has been funded by: ORAU program at Nazarbayev University through grants LIFESTART (PI: Daniele Tosi) and FOSTHER (PI: Carlo Molardi); ANR project NanoSlim (ANR-17-17-CE08-0002); FCT – Fundação para a Ciência e a Tecnologia, I.P., in the scope of the framework contract foreseen in the numbers 4, 5 and 6 of the article 23, of the Decree-Law 57/2016, of August 29, changed by Law 57/2017, of July 19, and when applicable co-funded by FEDER—PT2020 partnership agreement under the project UID/CTM/50025/2019. Tiago Paixão was funded by Fundação para a Ciência e Tecnologia (FCT) for the grant with the references PD/BD/128265/2016.

Conflicts of Interest: The authors declare no conflict of interest.

References

1. Othonos, A.; Kalli, K. *Fiber Bragg Gratings: Fundamentals and Applications in Telecommunications and Sensing*; Artech House: Boston, MA, USA, 1999.
2. Erdogan, T. Fiber grating spectra. *J. Light. Technol.* **1997**, *15*, 1277–1294. [CrossRef]
3. Liaw, S.K.; Ho, K.P.; Chi, S. Dynamic power-equalized EDFA module based on strain tunable fiber Bragg gratings. *IEEE Photonics Technol. Lett.* **1999**, *11*, 797–799. [CrossRef]
4. Chow, J.; Town, G.; Eggleton, B.; Ibsen, M.; Sugden, K.; Bennion, I. Multiwavelength generation in an erbium-doped fiber laser using in-fiber comb filters. *IEEE Photonics Technol. Lett.* **1996**, *8*, 60–62. [CrossRef]
5. Kersey, A.D.; Davis, M.A.; Patrick, H.J.; LeBlanc, M.; Koo, K.P.; Askins, C.G.; Putnam, M.A.; Friebele, E.J. Fiber grating sensors. *J. Light. Technol.* **1997**, *15*, 1442–1463. [CrossRef]
6. Liou, C.L.; Wang, L.A.; Shih, M.C. Characteristics of hydrogenated fiber Bragg gratings. *Appl. Phys. A* **1997**, *64*, 191–197. [CrossRef]
7. Liao, C.R.; Wang, D.N. Review of femtosecond laser fabricated fiber Bragg gratings for high temperature sensing. *Photonic Sens.* **2013**, *3*, 97–101. [CrossRef]
8. Mihailov, S.J.; Grobnic, D.; Smelser, C.W.; Lu, P.; Walker, R.B.; Ding, H. Bragg grating inscription in various optical fibers with femtosecond infrared lasers and a phase mask. *Opt. Mater. Express* **2011**, *1*, 754–765. [CrossRef]
9. Iadicicco, A.; Campopiano, S.; Cutolo, A.; Giordano, M.; Cusano, A. Refractive index sensor based on microstructured fiber Bragg grating. *IEEE Photonics Technol. Lett.* **2005**, *17*, 1250–1252. [CrossRef]
10. Jovanovic, N.; Åslund, M.; Fuerbach, A.; Jackson, S.D.; Marshall, G.D.; Withford, M.J. Narrow linewidth, 100 W cw Yb 3+-doped silica fiber laser with a point-by-point Bragg grating inscribed directly into the active core. *Opt. Lett.* **2007**, *32*, 2804–2806. [CrossRef]
11. Leal-Junior, A.; Frizera, A.; Marques, C.; Pontes, M.J. Mechanical properties characterization of polymethyl methacrylate polymer optical fibers after thermal and chemical treatments. *Opt. Fiber Technol.* **2018**, *43*, 106–111. [CrossRef]

12. Pugliese, D.; Konstantaki, M.; Konidakis, I.; Ceci-Ginistrelli, E.; Boetti, N.G.; Milanese, D.; Pissadakis, S. Bioresorbable optical fiber Bragg gratings. *Opt. Lett.* **2018**, *43*, 671–674. [CrossRef] [PubMed]
13. Yan, A.; Huang, S.; Li, S.; Chen, R.; Ohodnicki, P.; Buric, M.; Lee, S.; Li, M.J.; Chen, K.P. Distributed optical fiber sensors with ultrafast laser enhanced Rayleigh backscattering profiles for real-time monitoring of solid oxide fuel cell operations. *Sci. Rep.* **2017**, *7*, 9360. [CrossRef] [PubMed]
14. Parent, F.; Loranger, S.; Mandal, K.K.; Iezzi, V.L.; Lapointe, J.; Boisvert, J.S.; Baiad, M.D.; Kadoury, S.; Kashyap, R. Enhancement of accuracy in shape sensing of surgical needles using optical frequency domain reflectometry in optical fibers. *Biomed. Opt. Express* **2017**, *8*, 2210–2221. [CrossRef] [PubMed]
15. Monet, F.; Loranger, S.; Lambin-Iezzi, V.; Drouin, A.; Kadoury, S.; Kashyap, R. The ROGUE: A novel, noise-generated random grating. *Opt. Express* **2019**, *27*, 13895–13909. [CrossRef] [PubMed]
16. Beisenova, A.; Issatayeva, A.; Sovetov, S.; Korganbayev, S.; Jelbuldina, M.; Ashikbayeva, Z.; Blanc, W.; Schena, E.; Sales, S.; Molardi, C.; et al. Multi-fiber distributed thermal profiling of minimally invasive thermal ablation with scattering-level multiplexing in MgO-doped fibers. *Biomed. Opt. Express* **2019**, *10*, 1282–1296. [CrossRef] [PubMed]
17. Beisenova, A.; Issatayeva, A.; Korganbayev, S.; Molardi, C.; Blanc, W.; Tosi, D. Simultaneous distributed sensing on multiple MgO-doped high scattering fibers by means of scattering-level multiplexing. *J. Light. Technol.* **2019**, *37*, 3413–3421. [CrossRef]
18. Froggatt, M.; Moore, J. High-spatial-resolution distributed strain measurement in optical fiber with Rayleigh scatter. *Appl. Opt.* **1998**, *37*, 1735–1740. [CrossRef]
19. Blanc, W.; Mauroy, V.; Nguyen, L.; Shivakiran Bhaktha, B.N.; Sebbah, P.; Pal, B.P.; Dussardier, B. Fabrication of rare earth-doped transparent glass ceramic optical fibers by modified chemical vapor deposition. *J. Am. Ceram. Soc.* **2011**, *94*, 2315–2318. [CrossRef]
20. Marques, C.; Leal-Junior, A.; Min, R.; Domingues, M.; Leitão, C.; Antunes, P.; Ortega, B.; André, P. Advances on polymer optical fiber gratings using a KrF pulsed laser system operating at 248 nm. *Fibers* **2018**, *6*, 13. [CrossRef]
21. Soller, B.J.; Wolfe, M.; Froggatt, M.E. Polarization resolved measurement of Rayleigh backscatter in fiber-optic components. In Proceedings of the National Fiber Optic Engineers Conference, Anaheim, CA, USA, 6 March 2005; p. NWD3.
22. Molardi, C.; Korganbayev, S.; Blanc, W.; Tosi, D. Characterization of a nanoparticles-doped optical fiber by the use of optical backscatter reflectometry. In Proceedings of the SPIE Photonics Asia, Advanced Sensor Systems and Applications VIII, Beijing, China, 11–13 October 2018; Volume 10821, p. 1082121.
23. Lizárraga, N.; Puente, N.P.; Chaikina, E.I.; Leskova, T.A.; Méndez, E.R. Single-mode Er-doped fiber random laser with distributed Bragg grating feedback. *Opt. Express* **2009**, *17*, 395–404. [CrossRef] [PubMed]
24. Koeppel, M.; Werzinger, S.; Ringel, T.; Bechtold, P.; Thiel, T.; Engelbrecht, R.; Bosselmann, T.; Schmauss, B. Combined distributed Raman and Bragg fiber temperature sensing using incoherent optical frequency domain reflectometry. *J. Sens. Sens. Syst.* **2018**, *7*, 91–100. [CrossRef]
25. Xu, J.; Dziong, Z.; Cabani, A. Simultaneous temperature sensing using distributed cascading fiber Bragg grating-based single-ended Brillouin optical time-domain analyzer. *Laser Phys.* **2018**, *28*, 125101. [CrossRef]
26. Lu, P.; Grobnic, D.; Mihailov, S.J. Characterization of the birefringence in fiber Bragg gratings fabricated with an ultrafast-infrared laser. *J. Light. Technol.* **2007**, *25*, 779–786. [CrossRef]
27. Oh, S.T.; Han, W.T.; Paek, U.C.; Chung, Y. Discrimination of temperature and strain with a single FBG based on the birefringence effect. *Opt. Express* **2004**, *12*, 724–729. [CrossRef] [PubMed]
28. Van Roosbroeck, J.; Ibrahim, S.K.; Lindner, E.; Schuster, K.; Vlekken, J. Stretching the limits for the decoupling of strain and temperature with FBG based sensors. In Proceedings of the 24th International Conference on Optical Fibre Sensors, Curitiba, Brazil, 28 September–2 October 2015; Volume 9634, p. 96343S.
29. Caucheteur, C.; Guo, T.; Albert, J. Polarization-assisted fiber Bragg grating sensors: Tutorial and review. *J. Light. Technol.* **2016**, *35*, 3311–3322. [CrossRef]